

# Decline of Subpolar North Atlantic Circulation During the 1990s

Sirpa Häkkinen<sup>1\*</sup> and Peter B. Rhines<sup>2</sup>

Observations of sea surface height reveal that substantial changes have occurred over the past decade in the mid- to high-latitude North Atlantic Ocean. TOPEX/Poseidon altimeter data show that subpolar sea surface height increased during the 1990s, and the geostrophic velocity derived from altimeter data exhibits declining subpolar gyre circulation. Combining the data from earlier satellites, we find that subpolar circulation may have been weaker in the late 1990s than in the late 1970s and 1980s. Direct current-meter observations in the boundary current of the Labrador Sea support the weakening circulation trend of the 1990s and, together with hydrographic data, show that the mid- to late 1990s decline extends deep in the water column. Analysis of the local surface forcing suggests that the 1990s buoyancy forcing has a dynamic effect consistent with altimetric and hydrographic observations: A weak thermohaline forcing allows the decay of the domed structure of subpolar isopycnals and weakening of circulation.

Extreme fluctuations in atmospheric forcing of the subpolar zone of the North Atlantic Ocean, reflected by the North Atlantic Oscillation (NAO), have occurred over the past 30 years (1). These changes have demonstrably affected the water column and ocean circulation, as we show here with altimetry and in situ measurements.

The subpolar gyre of the North Atlantic circulates cyclonically between 50° and 65°N and contains strong boundary currents. It is a region of intense interaction between ocean and atmosphere: Wintertime cold winds remove heat at rates of several hundred watts per square meter, resulting in deep convection reaching as far as 2500 m below the surface. Newly formed subpolar waters combine with dense Nordic Sills overflows to provide the origins of North Atlantic Deep Water (NADW).

The subpolar North Atlantic undergoes a prominent decadal-to-century variability in its hydrographic properties (2–8). During the 1990s, in situ data from the Labrador Sea show decreased deep convection since 1996. This period of strong hydrographic change overlaps the TOPEX/Poseidon mission, which provides an opportunity to derive large-scale variability in the subpolar North Atlantic. Recent studies using TOPEX/Poseidon data have documented large changes between the early and later 1990s (9–11). These changes have been interpreted as being driv-

en by a shift in the NAO that took place in the winter of 1995–1996, moving the location of the subpolar frontal system (11). In addition, long-term hydrographic measurements from the eastern subpolar gyre show a decreasing trend, implying variation in southward-flowing deep water masses and extending back several decades (12).

Satellite observations of sea surface height (SSH) variations are usually interpreted in terms of heat storage, which at temperate latitudes and tropics is mainly determined by (adiabatic) vertical movement of isopycnals due to local and/or remotely forced dynamics. Toward high latitudes, SSH is affected by an increasing salinity contribution to seawater density and, owing to decreasing density stratification, by an increasingly barotropic (depth-independent) flow structure. In our study, the interpretation of SSH changes depends on the relative contribution of dynamics and local heat flux to heat storage in the subpolar gyre, where strong surface cooling can modify the stratification down to the deepest water masses. The dynamic impact of changes in ocean heat storage depends on their depth penetration, with deeper thermal anomalies bearing more potential energy and more baroclinic transport. For this reason, in situ current and hydrographic observations are important in validating inferences from altimetry data.

**Altimetry data analysis.** We use the archived 1°-resolution TOPEX/Poseidon data, which has been combined with ERS-1/2 data into the NASA Pathfinder data set. The Pathfinder data set also includes the Seasat and Geosat data, which are referenced to TOPEX. The height fields are validated against the

World Ocean Circulation Experiment (WOCE) global tide gauge network and the inverse barometric effect has been removed; various atmospheric corrections have also been applied. The accuracy of the TOPEX/Poseidon altimeter is about 4 cm, whereas that of Seasat and Geosat is on the order of 10 cm or more. The altimeter cannot resolve narrow currents lying close to coasts or ice cover.

Climatological SSH in the North Atlantic is low in the cyclonic subpolar gyre and high in the anticyclonic subtropical gyre. This surface topography reflects the thermocline structure and the sense of rotation of the gyres. We used empirical orthogonal function (EOF) analysis to investigate the monthly anomalies superimposed on this climatological state. The leading EOF mode of the SSH from the TOPEX/Poseidon-ERS-1-2 data (explaining 11.1% of the variance) has a spatial pattern of opposing sign SSH anomalies located over the Gulf Stream and over the western and northern side of the subpolar gyre (Fig. 1). The time series of this pattern displays a decade-long trend. PC1 and EOF1 jointly describe an increasing SSH over the subpolar gyre but decreasing SSH over the Gulf Stream. The trend in the subpolar gyre ranges from 4 to 9 cm/decade, greatest in the Irminger Sea. This could suggest changes in the convective processes driven by orographic winds or cooling in the wake of Greenland, as has been stressed recently (13). The dynamic height anomaly (referenced to 1000 m) calculated from hydrographic observations (Fig. 1) (fig. S3, Bedford Institute of Oceanography AR7/W section) compares well with the actual altimeter SSH anomaly from the central Labrador Sea, as also shown in Fig. 1B.

Altimetric SSH anomalies, whatever their origin, balance geostrophic velocity anomalies, in part corresponding to changes in gyre circulation. The geostrophic velocities are computed from SSH smoothed once by Laplacian filter. Because SSH variability for the period May 1992 to April 2002 is dominated by a trend, a linear trend (from the least-squares method) in the geostrophic velocity field is recovered. Trend vectors suggest a weakening gyre circulation because the subpolar pattern resembles the mean gyre circulation inferred from hydrography and velocity observations but with opposite sign (Fig. 2). Off the Labrador Coast the velocity decline is 1 to 1.5 cm/s per decade, which, with approximate width of 500 km and depth of 1500 m, would correspond to about 7 to 10 Sv ( $1 \text{ Sv} = 10^6 \text{ m}^3/\text{s}$ ) change in transport. Observational estimates have roughly 40 Sv total transport in the Labrador Sea boundary current; thus, the decline is a significant fraction of the mean flow. The course estimate is consistent with the interannual transport variability of the Labrador Boundary Current from 1992 to 1998 computed

<sup>1</sup>NASA Goddard Space Flight Center, Code 971, Greenbelt, MD 20771, USA. <sup>2</sup>University of Washington, Box 357940, Seattle, WA 98195, USA.

\*To whom correspondence should be addressed. E-mail: sirpa.hakkinen@nasa.gov

using AR7/W hydrography and SSH gradient along two altimeter tracks (9).

The trend vectors (Fig. 2) correspond well with the shape of the western subpolar gyre; the mean circulation involves boundary currents along the Iceland-Scotland Ridge and around the Labrador Sea. The total northward flow has components in mid-basin, along the Reykjanes Ridge toward Iceland, and also in the eastern basin, feeding the northward flow of warm Atlantic water to the Nordic seas. Observations using drifting buoys and deep neutrally buoyant floats (drifting at fixed pressure level; called

RAFOS floats) all support the multiple and time-variable pathways of northward circulation in this region, with strong recirculation gyres. In particular, isopycnal RAFOS floats show circulation at about 600 m depth resembling (with opposite direction) our surface trend map, with much of the Gulf Stream water recirculating within the western subpolar gyre rather than extending far to the east (14–18).

The *t* test for the significance of the trend is performed for both vector components separately, and the larger one is chosen to indicate the significance of the trend

vector. The resulting distribution of *t* test values shows the trend to be more significant in the subpolar gyre than in the subtropics. This finding suggests that the subpolar ocean is particularly suitable for detecting decadal climate signals on basin scales. The same signal is likely to exist elsewhere in the North Atlantic, but the signal-to-noise ratio is poor.

Altimeter data are also available for two months in 1978 (Seasat) and for nearly 4 years during the 1980s (Geosat). In an EOF analysis we can combine all the satellite measurements to

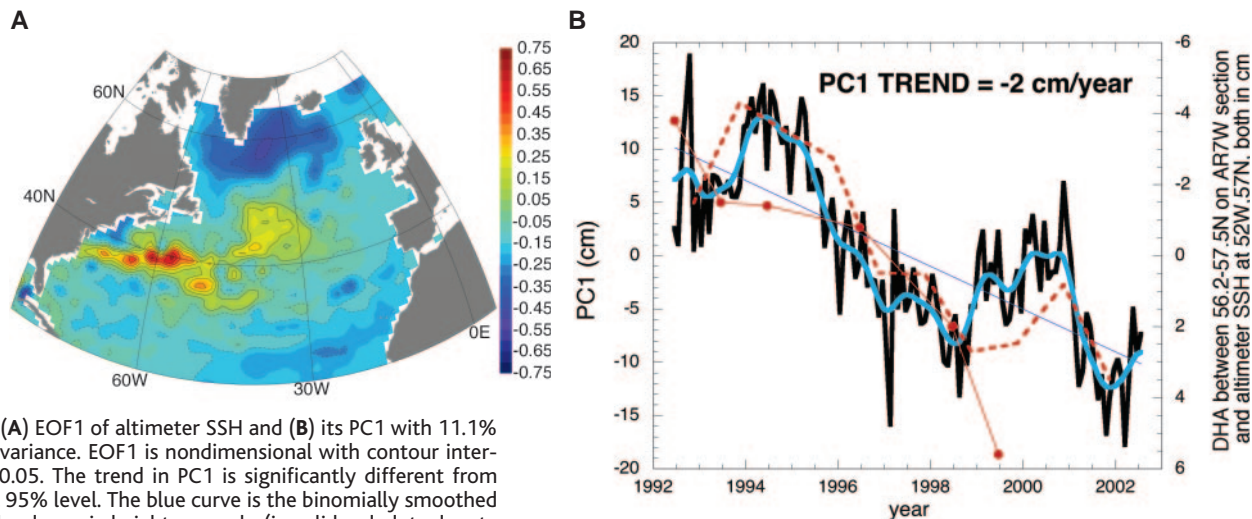
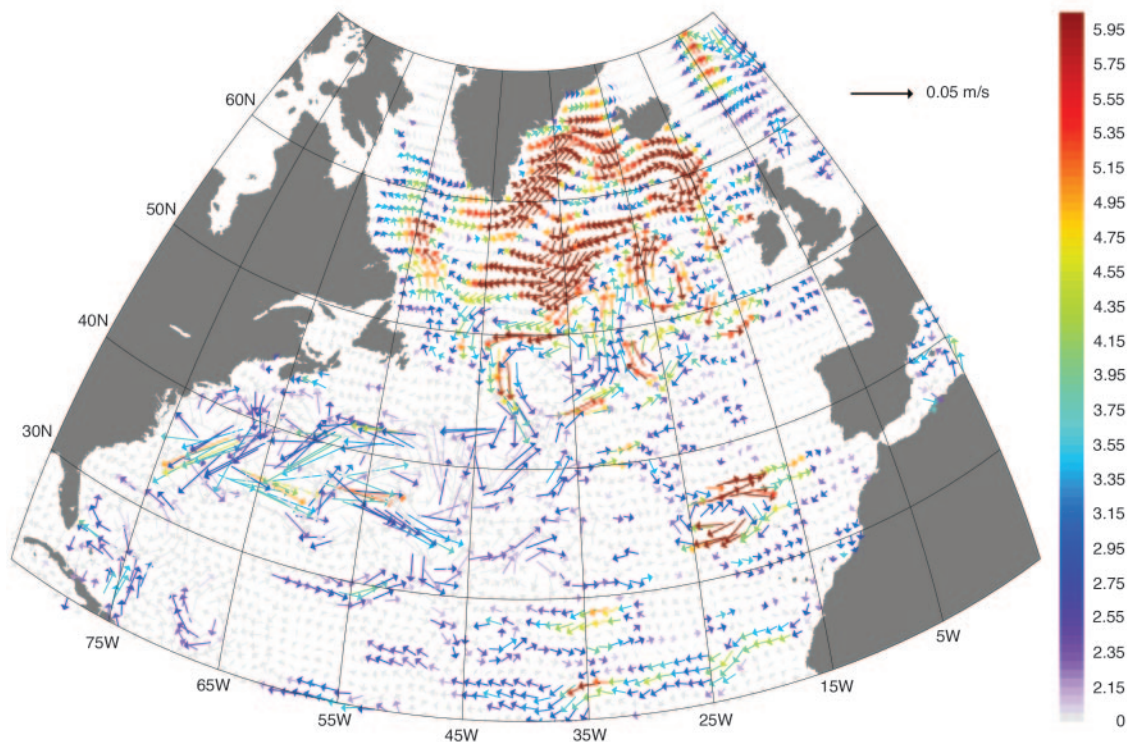


**Fig. 1.** (A) EOF1 of altimeter SSH and (B) its PC1 with 11.1% of the variance. EOF1 is nondimensional with contour interval of 0.05. The trend in PC1 is significantly different from zero at 95% level. The blue curve is the binomially smoothed PC1. The dynamic height anomaly (in solid red; dots denote data points of the time series) computed in the central Labrador Sea (average from 56.2° to 57.5°N along the WOCE AR7/W section across the Labrador Sea from Newfoundland to Greenland) is shown in (B) with its axis on right. The altimeter SSH anomaly at 52°W, 57°N (12-month May-to-April average; dashed red) in the central Labrador gives a similar result of about 8 cm from 1994 to 2002.

**Fig. 2.** Trend of the geostrophic velocities (m/s per decade) derived from altimeter data for the period May 1992 to June 2002. Vector colors represent the *t* test value. Values above 2.0 are significant at the 95% level; only vectors above this significance level are shown. Velocities above 0.05 m/s per decade are truncated.



infer the gyre strength (assuming that the EOF is stable) at these separate time intervals. The first EOF pattern (EOF1) of the geostrophic velocity field contains 9.4% of the total variance when the velocity components are normalized by the standard deviation of the current speed anomalies (i.e., reducing the Gulf Stream “dominance” that is apparent in fig. S1 of early TOPEX and Geosat velocities) and then smoothed temporally by four binomial filters. (The variance of the first mode increases to 16% for the TOPEX period with nearly identical spatial pattern of vectors.) EOF1 (Fig. 3A) displays nearly the same pattern as the trend map (Fig. 2) but with opposite sign, because the EOF1 currents are chosen to align with the climatological circulation.

The corresponding time series (first principal component PC1; Fig. 3B) shows that the Seasat and Geosat periods appear to be about the same strength, but the 1990s data show a large amplitude change, with a maximum in the beginning of the 1990s (during years with a high NAO index) and the lowest strength in the late 1990s (during years with a negative or

moderate NAO index). We caution that Seasat and Geosat have considerably larger errors than TOPEX/Poseidon. However, differencing the 44 months of the Geosat data and the first 44 months of the Pathfinder ERS-TOPEX data (fig. S1) yields the same large-scale pattern as in the EOF analysis. The coherence over the large basin scales supports the significance of the differences in the gyre strength indicated by the EOF analysis.

**Current-meter observations.** Uncertainty about altimetric data accuracy in boundary currents can be alleviated where direct current measurements are available. In October 1996, the second author and J. R. N. Lazier of the Bedford Institute of Oceanography deployed a subsurface mooring, M1244, for 19 months at the 2800-m isobath (55.49°N, 53.655°W) on the Labrador continental slope (Fig. 3A). This location is the core of the boundary current carrying Denmark Strait Overflow Water in the lower 500 m, and it also captured much of the structure in the Northeast Atlantic Deep Wa-

ter, Labrador Sea Water, and Irminger Sea Water above; the principal water masses of the region and dense overflows from the Nordic seas all pass through this region. The vertical structure of the boundary current is remarkably barotropic, considering its baroclinic origins. The time series (Fig. 4) show that the upper level circulation (here from 200 m depth) decreases about 25% over the length of the record, approximately in parallel with the decrease in the PC1 time series. Taken alone, this record would not establish a longer trend, yet it supports the altimetric picture of a gyre weakening in the mid-1990s. Figure 3B shows that the general downward trend occurs over the full water column, between 200 and 2750 m. This suggests that the trend in the altimeter observations is representative of the evolution in all the major water masses of the subpolar gyre. A contribution to the trend in the deepest water masses may also come from farther north: The Faeroe-Shetland Channel contribution to the NADW overflow has experienced a down-

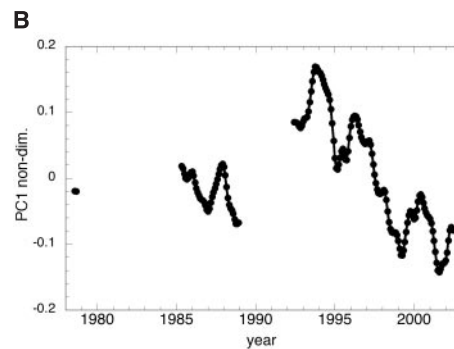
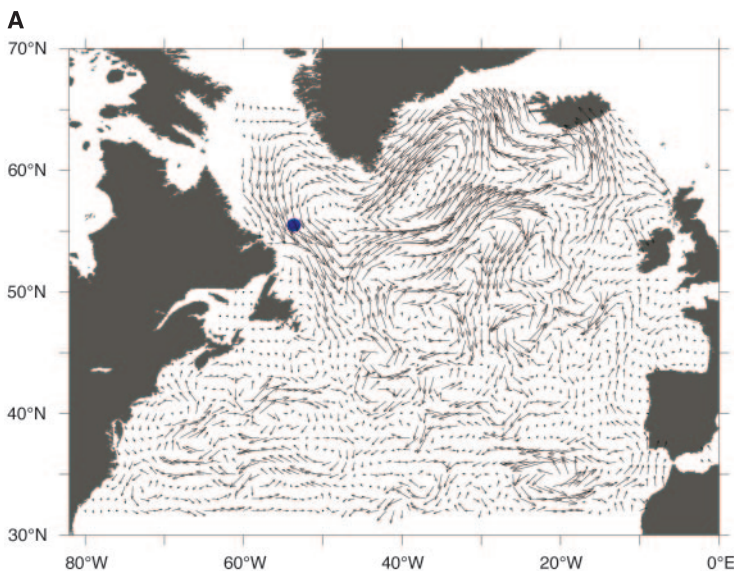
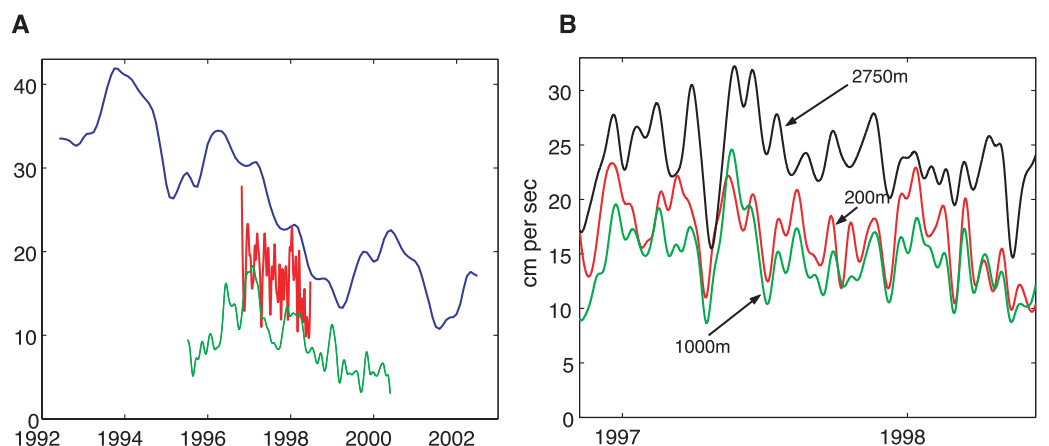


**Fig. 3.** (A) EOF1 of the geostrophic velocity field derived from the altimeter data with 9.4% of the variance. The vectors are nondimensional because of normalization of each velocity component by the standard deviation of the current speed anomaly. The blue dot denotes the location of current-meter mooring M1244. (B) PC1 of the geostrophic velocity field in nondimensional units.

**Fig. 4.** (A) Current-meter records from the subpolar Atlantic, with the time series of the first principal component of the TOPEX altimetry (blue curve). The 200-m level along-isobath velocity at the 2850-m isobath in the Labrador Sea boundary current shows a downward trend over 19 months (red curve; because of differing units, the slopes of velocity and PC1 curves cannot be compared). The along-isobath velocity, measured 10 m above the bottom at 1000 m depth, site M3 (green curve), 45 km to the southwest, has a similar, more marked downward trend after 1996. The y axis is in arbitrary units. (B) The vertical structure at the mooring on the 2800-m isobath shows similar downward trend at all depths, including the deep circulation and water masses from the Denmark Strait Overflow and Iceland-Scotland Overflow.



ward trend since 1996 based on direct ADCP current measurements and inferred from hydrography to have continued 50 years into the past (12).

In addition to our current record above, a longer record, from 1979 to the present (M3, Fig. 4) from the 1000-m isobath, upslope from the M1244 (maintained by the Bedford Institute of Oceanography), suggests that the mid-1990s were unusually energetic relative to the 1980s and late 1990s. The time series of the along-isobath current and temperature (fig. S2) show the decadal variation of Labrador Sea Water temperature as well as a mid-1990s maximum in current. The deceleration from mid-1996 to 2000 resembles the altimetric record. The currents before the 1993–1996 data gap show little annual or interannual variability. This would be consistent with the unusually strong circulation in the early to mid-1990s.

**Possible causes for the 1990s decline in the subpolar circulation.** The 1990s climate in the North Atlantic is dominated by a large shift in NAO intensity, from an extreme high index in the early 1990s to a low index in 1996. NAO intensity influences both the buoyancy and wind stress curl over the subpolar ocean. Changes of the gyre circulation can originate from several sources: the effects of wind stress, local air-sea buoyancy forcing, and distant air-sea interaction propagated into the region by the circulation itself, as

well as the interplay between fast, barotropic response to wind stress curl changes (19, 20) and barotropic gyre response to the baroclinic overflows entering the region (21). There are indications of enhancement of both cyclonic circulation and the meridional overturning cell (MOC) following cold, windy winters seen in distant boundary currents (22, 23), consistent with our results, but in a reverse sense. Despite the complexity of the problem, buoyancy and wind stress variability can be analyzed to infer their dynamic influences on the subpolar gyre. These inferences are offered as possible explanations but not as a proof for one mechanism over another.

To explore possible causes of the gyre changes, we use EOF analysis applied to the wind stress curl and net heat flux (from National Center for Environmental Prediction/National Center for Atmospheric Research reanalysis) for the period 1978–2002. The spatial patterns of the leading EOF mode for the wind stress curl and net heat flux are shown in Fig. 5, A and B, where the sign convention is such that a positive curl corresponds to cyclonic circulation and a positive heat flux is upward.

The time series (PC1) associated with the spatial patterns in Fig. 5, A and B, of the wind stress curl and net heat flux EOF1s are plotted against the altimetric velocity field PC1 in Fig. 5C along with the wintertime (November to April) NAO index. There are several features to observe:

1) As noted earlier, NAO has fluctuated wildly but has returned to positive range by the late 1990s. However, the air-sea heat flux pattern normally associated with the NAO has not developed, as the Atlantic storm track has migrated east since 1995 (24).

2) The relationship between NAO and the corresponding wind stress curl change is often (but not always, as seen from Fig. 5C) such that positive NAO results in an anticyclonic wind stress curl anomaly, thus in an anticyclonic circulation anomaly in the subpolar gyre (19, 20, 25–27).

3) Wind stress curl and heat flux PC1s both contain a downward trend since 1994, but the wind stress curl PC1 has large fluctuations similar to the NAO index for the obvious reason that it reflects the NAO variability.

4) Only the net heat flux and geostrophic velocity PC1s follow the overall downward trend in the 1990s, with only modest fluctuations about the trend.

Property 2 and the combined information from Fig. 5, A and C, imply that the wind stress curl anomaly over the subpolar gyre in the 1990s evolves toward a cyclonic state, and thus would give more cyclonic spin to the gyre if the ocean response is of barotropic nature. However, the altimeter and current-meter results suggest the opposite, a decay of the cyclonic gyre (i.e., anticyclonic anomaly). On the other hand, model studies suggest that the baroclinic response to the

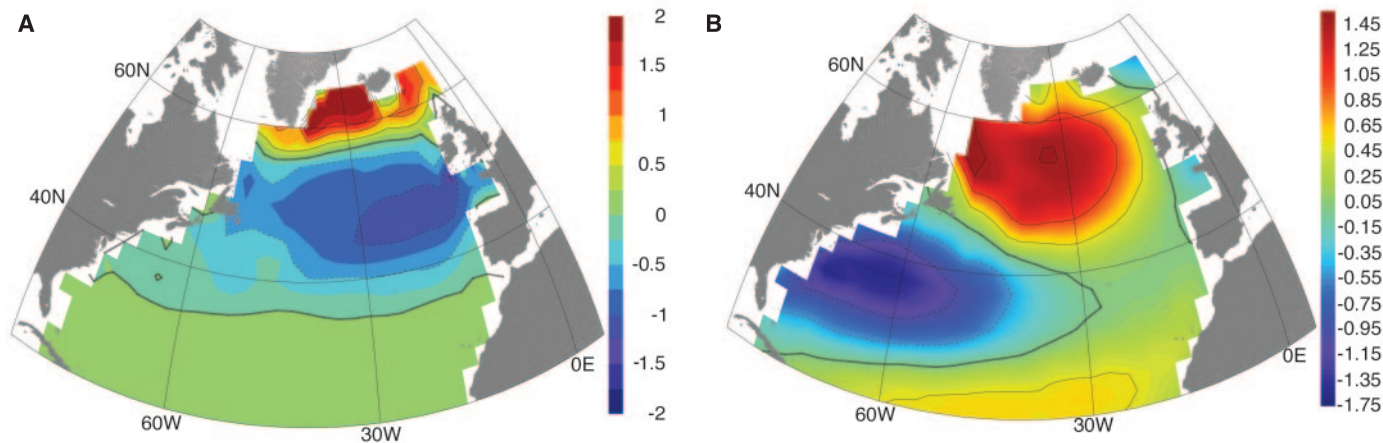
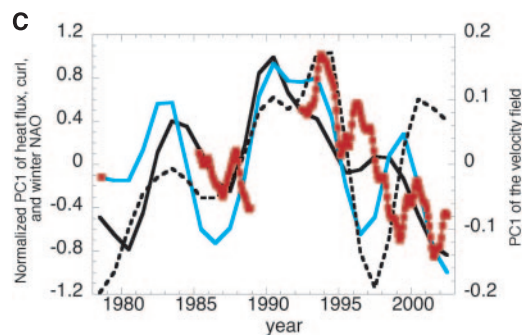


**Fig. 5.** Wind stress curl (A) and net heat flux (B) EOF1 explaining 19.2% and 19.4% of the variance, respectively (values are nondimensional). Positive values denote cyclonic curl and mean upward flux (heat loss from the ocean), respectively. (C) Geostrophic velocity PC1 (red squares) plotted against winter NAO (dashed black) and normalized PC1 of wind stress curl (blue) and of heat flux (black solid).



wind stress curl changes is a delayed process and would retard the existing cyclonic circulation. We would expect this influence to manifest itself with large reversals in PC1 of the geostrophic velocity like the variations in the curl PC1 or NAO with a 3- to 5-year delay. Figure 5C shows that there are peaks in geostrophic velocity PC1 with such a delay, but they are small relative to the overwhelming background trend.

Property 3 of the continuous weakening of the subpolar air-sea heat loss is consistent with the observations that deep convective conditions in the Labrador Sea have been absent since the early 1990s. Although changes in advection of heat can have as much as 50% effect on the subpolar heat storage changes (10), the local heat flux changes are still important, particularly in forcing deep convection. Because deep convection maintains a cold core around which lighter water masses circulate, cessation of deep convection would lead to a decaying baroclinic gyre. This decaying cold core of the Labrador Gyre from 1992 to 2002 is observable in the dynamic height increase (using WOCE section AR7/W), which is about 6 cm relative to 1000db (Fig. 1A) (fig. S3) and comparable with the altimeter SSH change. The strong height gradient associated with boundary currents is important to inferences of circulation; this is seen in the hydrography (fig. S3). Evidence from the hydrographic data together with the 1990s heat flux trend is supportive of a connection between convective forcing and the observed decline in the gyre strength. It might not have been the case if wind-driven barotropic circulation or overflow-driven circulation variability were dominant causes.

**Conclusions.** Altimetric geostrophic circulation observations and supporting deep-sea current-meter observations suggest significant changes over the last two decades, with increasing SSH and weakening subpolar gyre circulation in the 1990s. By comparing the dynamic consequences of three mechanisms, buoyancy forcing and barotropic and baroclinic response to local wind stress curl, we find that the gyre weakening in the 1990s is not attributable to local wind stress changes associated with NAO. The weakening-gyre scenario of the 1990s parallels the warming in the central subpolar gyre, which is the well-observed relaxation of the water column following the intense winter convection period of 1989–1994. The lack of deep convection is the oceanic response to the local buoyancy forcing, which has mimicked low-NAO heat fluxes even though the index itself has reversed itself twice during the 1990s.

Because we lack SSH data before 1978, we cannot determine whether the 1990s slowing gyre is a part of a decadal cycle or the beginning of a longer term trend. Because Labrador Sea processes are intimately linked to the meridional overturning circulation, involving both intermediate-depth and deep waters, these observations of rapid climatic

changes over one decade may merit some concern for the future state of the MOC. Continuation of the altimeter missions will allow us to follow the evolution of this subpolar signal and its influence on the North Atlantic. Field observations of the subsurface oceanic circulation, hydrography, and ice cover (28) will be of great importance in establishing the origin of these climate shifts.

#### References and Notes

1. J. W. Hurrell, *Science* **269**, 676 (1995).
2. R. R. Dickson *et al.*, *Nature* **416**, 832 (2002).
3. J. R. N. Lazier *et al.*, *Deep-Sea Res.* **49**, 1819 (2002).
4. C. Deser, M. L. Blackmon, *J. Clim.* **6**, 1743 (1993).
5. G. Reverdin, D. Cayan, Y. Kushnir, *J. Geophys. Res.* **102**, 8505 (1997).
6. I. M. Belkin, S. Levitus, J. Antonov, S.-A. Malmberg, *Prog. Oceanogr.* **41**, 1 (1998).
7. R. G. Curry, M. S. McCartney, *J. Phys. Oceanogr.* **31**, 3374 (2001).
8. R. R. Dickson, J. Meincke, S.-A. Malmberg, A. J. Lee, *Prog. Oceanogr.* **20**, 103 (1988).
9. G. Han, C. L. Tang, *J. Phys. Oceanogr.* **31**, 199 (2001).
10. N. Verbrugge, G. Reverdin, *J. Phys. Oceanogr.* **33**, 964 (2003).
11. M. K. Flatau, L. Talley, P. P. Niiler, *J. Clim.* **16**, 2355 (2003).
12. B. Hansen, W. Turrell, S. Osterhus, *Nature* **411**, 927 (2001).
13. R. S. Pickart *et al.*, *Nature* **424**, 152 (2003).
14. A. S. Bower *et al.*, *Nature* **419**, 603 (2002).
15. M. A. White, K. J. Heywood, *J. Geophys. Res.* **100**, 24931 (1995).
16. J. Cuny, P. B. Rhines, P. P. Niiler, S. Bacon, *J. Phys. Oceanogr.* **32**, 627 (2002).
17. D. M. Fratantoni, *J. Geophys. Res.* **106**, C1022067 (2001).
18. The RAFOS floats (14) highlight meridional pathways at depths ranging from near-surface to 1500 m. White and Heywood (15) argued from early altimeter data that changing winds can shift the site of northward flow; Cuny *et al.* (16) and Fratantoni (17) compared surface drifter data with satellite altim-

- etry, yet data density was not sufficient to show significant changes between the 1990s and 1980s.
19. S. Häkkinen, *J. Geophys. Res.* **106**, 13837 (2001).
  20. C. Eden, J. Willebrand, *J. Clim.* **14**, 2266 (2001).
  21. R. Döscher, C. W. Böning, P. Herrmann, *J. Phys. Oceanogr.* **24**, 2306 (1994).
  22. W. M. Smethie, R. A. Fine, *Deep-Sea Res.* **48**, 189 (2001).
  23. Mapping the distribution of natural and human-made trace chemicals is an "accurate" way to view the MOC [see, e.g., (22)].
  24. The "normal" heat flux pattern corresponding to NAO has the Labrador Sea out of phase with the Greenland-Norwegian Sea (29), but the eastward migration of the Icelandic Low has altered this relationship since 1995.
  25. P. B. Rhines, *J. Fluid Mech.* **37**, 161 (1969).
  26. R. J. Greatbatch, A. D. Goulding, *J. Phys. Oceanogr.* **19**, 572 (1989).
  27. Wind-driven currents are set up by propagation of topographic Rossby waves along f/h (Coriolis frequency/total depth) contours, eventually approximating a topographic-Sverdrup balance. This produces over a matter of a few weeks a single anticyclonic gyre, or "intergyre," centered at 50°N latitude, at the boundary between subpolar and subtropical gyres. The Mid-Atlantic Ridge dominates this f/h waveguide (25, 26).
  28. The Arctic-SubArctic Flux Program (ASOF) (<http://asof.npolar.no>) is an observational campaign bridging programs such as SEARCH and CLIVAR.
  29. R. R. Dickson *et al.*, *Prog. Oceanogr.* **38**, 241 (1996).
  30. Supported by the NASA Physical Oceanography Program (S.H.) and by the NOAA Arctic Research Office, Vetlesen Foundation, and the NSF Office of Polar Programs (P.B.R.). The Office of Naval Research and Bedford Institute of Oceanography supported the current-meter measurements. We thank J. R. N. Lazier, I. Yashayev, and J. Cuny for help with the subsurface ocean data, and D. Worthen for assistance with graphics.

#### Supporting Online Material

[www.sciencemag.org/cgi/content/full/304/5670/555/DC1](http://www.sciencemag.org/cgi/content/full/304/5670/555/DC1)  
Figs. S1 to S3

19 December 2003; accepted 20 March 2004

## Synfire Chains and Cortical Songs: Temporal Modules of Cortical Activity

Yuji Ikegaya,<sup>1\*</sup> Gloster Aaron,<sup>1\*</sup> Rosa Cossart,<sup>1</sup>  
Dmitriy Aronov,<sup>1</sup> Ilan Lampl,<sup>2</sup> David Ferster,<sup>2</sup> Rafael Yuste<sup>1†</sup>

How can neural activity propagate through cortical networks built with weak, stochastic synapses? We find precise repetitions of spontaneous patterns of synaptic inputs in neocortical neurons *in vivo* and *in vitro*. These patterns repeat after minutes, maintaining millisecond accuracy. Calcium imaging of slices reveals reactivation of sequences of cells during the occurrence of repeated intracellular synaptic patterns. The spontaneous activity drifts with time, engaging different cells. Sequences of active neurons have distinct spatial structures and are repeated in the same order over tens of seconds, revealing modular temporal dynamics. Higher order sequences are replayed with compressed timing.

The essence of cortical function is the propagation and transformation of neuronal activity by the cortical circuit (1). How activity can propagate through a network composed of weak, stochastic, and depressing synapses is, however, poorly understood (2–4). It has been proposed that sequences of synchronous activity ("synfire chains") propagate through

the cortical circuit with high temporal fidelity (5, 6). Synchronous summation of excitatory postsynaptic potentials (EPSPs) could ensure postsynaptic firing and the nonlinear gain caused by the spike threshold could preserve temporal fidelity, so reactivations of the same chain would result in exact repetitions of precise firing patterns (7). Repetitions of